

# A CURRENT-BASED OUTPUT FEEDBACK SLIDING MODE CONTROL FOR SPEED SENSORLESS INDUCTION MACHINE DRIVE USING ADAPTIVE SLIDING MODE FLUX OBSERVER

G. R. Arab Markadeh and J. Soltani\*

Department of Electrical and Computer Engineering, Isfahan University of Technology  
Isfahan, Iran, arab\_r@yahoo.com - j1234sm@cc.iut.ac.ir

\*Corresponding Author

(Received: January 26, 2004 - Accepted in Revised Form: June 1, 2006)

**Abstract** This paper presents a new adaptive Sliding-Mode flux observer for speed sensorless and rotor flux control of three-phase induction motor (IM) drives. The motor drive is supplied by a three-level space vector modulation (SVM) inverter. Considering the three-phase IM Equations in a stator stationary two axis reference frame, using the partial feedback linearization control and Sliding-Mode (SM) control, the rotor speed and rotor flux controllers are derived first. These controllers are capable of making the drive system states follow the system nominal trajectories in spite of the motor parameter uncertainties and external load torque disturbance. Then, based on the Lyapunov theory, a SM observer is developed in order to estimate the rotor flux, rotor speed and rotor resistance simultaneously. In addition, in order to satisfy the persistent excitation (P.E) condition, a low frequency low amplitude ac signal is superimposed to the rotor flux reference command. Finally, the validity and effectiveness of proposed control approach is verified by computer simulation.

**Key Words** Induction Machine, Sliding Mode Control, Adaptive, Output Feedback, Sliding Mode Observer, Speed Sensorless

**چکیده** این مقاله یک مشاهده گر جدید مد لغزشی شار برای کنترل سرعت و شار مغناطیسی روتور موتور درایو سه فاز القایی ارائه می کند. موتور درایو توسط یک اینورتر سه سطحی از نوع مدولاسیون فضای بردارهای فضایی ولتاژهای استاتور تغذیه می گردد. با در نظر گرفتن معادلات موتور القایی سه فاز در یک مختصات دو محوری ساکن استاتور و با بکارگیری روشهای کنترل خطی سازی ورودی خروجی و کنترل مد لغزشی، ابتدا کنترل کننده های سرعت روتور و شار روتور استخراج می گردند. این کنترل کننده ها قابلیت کنترل تعقیب مسیر حالت های نامی موتور را علیرغم وجود نا معینی ها در پارامترها و نیز اغتشاش گشتاور بار دارا می باشند. آنگاه بر پایه تئوری لیاپانوف، یک مشاهده گر مد لغزشی توسعه می یابد که شار، سرعت و مقاومت روتور را تخمین می زند. بعلاوه بمنظور برقراری شرط تحریک مداوم، یک سیگنال ac با دامنه و فرکانس کم به سیگنال شار مرجع روتور اضافه می گردد. در پایان، برقراری و موثر بودن روش کنترل پیشنهادی با شبیه سازی کامپیوتری شرح داده می شود.

## 1. INTRODUCTION

SM theory is one of the prospective control methodologies for IM flux and speed control because of its order reduction, disturbance rejection, strong robustness and particularly its simplicity of implementation by power converters [1,2]. SM observers have also robust features as SM controllers. So far, a few research reports have been reported for the speed and rotor flux estimation of the IM using an SM observer [3,4].

In [3], a PD type SM controller has been proposed to regulate the speed and the square of rotor flux magnitude of an IM. In addition, a SM observer is also derived to estimate the rotor flux vector components in a two-phase stationary reference frame. Tursini et al. in reference [4], have presented an SM observer for a three-phase 0.225kW rotor-flux field oriented IM to estimate the rotor speed. In fact, the SM observers developed in [3] and [4] are basically equal except that in [4], a criterion has also been

proposed for choosing the gains of the adaptive flux observer.

A closed loop current model SM flux observer has been proposed in [5] and used to estimate the rotor speed, rotor position and rotor flux vector components of a 5kW cage rotor IM in a fixed stator  $\alpha-\beta$ : axis reference frame. The rotor flux observer of [5] has two main drawbacks: First is that with constant rotor flux amplitude, it is not possible to detect the correct values of rotor time constant and rotor speed simultaneously [6,7]. This is due to the fact that we can not separate the speed and rotor time constant estimated errors from the stator variables in a steady state. Second is that, according to the equivalent control concept described in [5], the estimation of error of the speed and rotor time constant will only converge to zero if the stator currents and the rotor flux estimated errors also tend to zero. Therefore in transient conditions especially in the reaching phase condition of SM flux observer, the indirect-field orientation (IFO) control of the IM drive system may be lost.

To overcome the above problems, this paper presents the following research:

1. Considering the IM Equations in a  $\alpha-\beta$ : axis stationary reference frame, using the partial feedback linearization control, two input-output state variables are introduced and used to decouple the dynamics of IM torque and rotor flux magnitude.
2. By combining the SM control and Linear Quadratic (LQ) feedback control method, the composite rotor speed and rotor flux controllers are derived and create the merits for easy design, simplicity of implementation by power electronic devices, strong robustness with minimum chattering and no reaching phase.
3. A closed loop current model SM rotor flux observer is derived in order to provide the simultaneous estimation of rotor speed, rotor time constant and rotor flux vector components in a stator fixed two axis reference frame. The stability of the SM observer is proved by the Lyapunov theory. In addition, in order to satisfying the P.E condition and convergent behavior of the SM observer, a low frequency low amplitude ac signal is superimposed to the rotor flux reference command [8].
4. A three-level SV-based PWM inverter is

employed to feed the induction drive system. A so-called vector classification algorithm based on Artificial Neural Network (ANN), is applied to obtain the PWM inverter switching patterns and on-duration of power electronic devices [11]. This method reduces software and hardware complexity, decreases the computation time and increases the accuracy of the positioning switching instants.

## 2. SYSTEM DYNAMIC EQUATIONS

The fifth order model of the three-phase induction machines in a stationary  $\alpha-\beta$ : axis reference frame with stator currents, rotor speed and rotor flux as variables are defined by:

$$\frac{d}{dt} \begin{bmatrix} i_s \\ \phi_r \end{bmatrix} = \begin{bmatrix} A_{11} & A_{12} \\ A_{21} & A_{22} \end{bmatrix} \begin{bmatrix} i_s \\ \phi_r \end{bmatrix} + \begin{bmatrix} B_1 \\ 0 \end{bmatrix} v_s \quad (1)$$

$$\frac{d}{dt} \omega_m = -\frac{B_f}{J_m} \omega_m + \mu i_s^T J \phi - \frac{T_l}{J_m} \quad (2)$$

With

$$i_s = \begin{bmatrix} i_{ds} \\ i_{qs} \end{bmatrix}, \phi_r = \begin{bmatrix} \phi_{dr} \\ \phi_{qr} \end{bmatrix}, v_s = \begin{bmatrix} v_{ds} \\ v_{qs} \end{bmatrix}$$

$$A_{11} = -\left(\frac{R_s}{\sigma} + \beta M \alpha\right) I, A_{21} = M \alpha \alpha$$

$$A_{12} = \beta \left( \alpha I - \omega_r J \right), A_{22} = -\alpha I + \omega_r J$$

$$B_1 = \frac{I}{\sigma}, I = \begin{bmatrix} 1 & 0 \\ 0 & 1 \end{bmatrix}, J = \begin{bmatrix} 0 & -1 \\ 1 & 0 \end{bmatrix}$$

$$\alpha = \frac{R_r}{L_r}, \sigma = L_s \left( 1 - \frac{L_m^2}{L_s L_r} \right)$$

$$\mu = \frac{L_m}{J_m L_r}, \beta = \frac{L_m}{\sigma L_r}$$

where

$R_s$  and  $R_r$ : stator and rotor resistance

$L_s$  and  $L_r$ : stator and rotor inductance

$L_m$ : mutual inductance

$\sigma$ : leakage coefficient

$\alpha$ : reverse of the rotor time constant

$\omega_m$ : rotor mechanical angular speed

$\omega_r$ : rotor electrical angular speed

$J_m$ : moment of inertia

$B_f$ : friction coefficient

Using Equations 1 and 2, based on partial feedback linearization control, the following control inputs are introduced.

$$\begin{bmatrix} U_\phi \\ U_T \end{bmatrix} = T \begin{bmatrix} i_{ds} \\ i_{qs} \end{bmatrix} \quad (3)$$

with

$$T = \frac{1}{\Phi_r} \begin{bmatrix} \phi_{dr} & \phi_{qr} \\ -\Phi_r \phi_{qr} & \Phi_r \phi_{dr} \end{bmatrix}$$

Linking Equations 1-3, yields

$$\frac{d}{dt} \omega_m = -\frac{B}{J_m} \omega_m + \frac{K_T}{J_m} U_T - \frac{T_l}{J_m} \quad (4)$$

$$\frac{d}{dt} \Phi_r = -\frac{1}{\tau_r} \Phi_r + \frac{L_m}{\tau_r} U_\phi \quad (5)$$

where  $K_T = \frac{3P L_m}{4 L_r}$  and  $P$  is number of stator poles.

From Equations 4 and 5, the feedback-state variables  $U_T$  and  $U_\phi$ , can be used to control the rotor speed and rotor flux independently. However, in the perturbed condition, while the parameter uncertainties and the disturbance load torque occur, it is necessary to decouple the rotor flux dynamic from the rotor speed dynamic completely.

The way of doing that is explained in the subsequent section.

### 3. SLIDING-MODE CONTROLLER

**A. Purpose of Design** In this section, based on state-space Equations of the linear system and the introduced performance index, the general control concepts of the LQ feed back control is used to design a linear control to satisfy the IM dynamic system requirements. The pole placement method is an adequate way to meet this objection, if an optimal performance index is also considered.

The LQ feed back control method is easily able to determine the desired feed back gains to satisfy the requirements, however the method will not be able to conserve the responses as the nominal condition once parameter uncertainty and external load torque disturbance are present. in order to conserve the responses and reject the effects of the external disturbance and parameters uncertainties, the system controllers are designed by combining the classical LQ feed back control and SM control. Using these composite controllers, it will be shown that the rotor speed and rotor flux controllers are insensitive to uncertainties and external unknown load torque.

**B. Nominal System Control** The state Equations 4 and 5 in matrix form become

$$\dot{x} = Ax + bU(t) + d.T_l \quad (6)$$

where

$$A = \begin{bmatrix} -a_\omega & 0 \\ 0 & -a_\phi \end{bmatrix}, b = \begin{bmatrix} b_\omega & 0 \\ 0 & b_\phi \end{bmatrix}, U = \begin{bmatrix} U_T \\ U_\phi \end{bmatrix}$$

and

$$a_\omega = \frac{B}{J_m}, b_\omega = \frac{K_T}{J_m}, d = -\frac{1}{J_m}$$

$$a_\phi = \frac{1}{\tau_r}, b_\phi = \frac{L_m}{\tau_r}$$

For a desired rotor speed  $\omega_{ref}$  and a rotor flux magnitude,  $\Phi_{ref}$  the deviation form of Equation 6

can be derived as:

$$\dot{e} = Ae + bU(t) + f(t) \quad (7)$$

where

$$e = \begin{bmatrix} e_\omega & e_\phi \end{bmatrix}^T, \quad e_\omega = \omega_{rm} - \omega_{ref}$$

$$e_\phi = \Phi_r - \Phi_{ref}$$

and

$$f(t) = \begin{bmatrix} -\dot{\omega}_{ref} + a_\omega \omega_{ref} + d.T_1 \\ \dot{\Phi}_{ref} + a_\phi \Phi_{ref} \end{bmatrix} = \begin{bmatrix} f_\omega(t) \\ f_\phi(t) \end{bmatrix}$$

In view of the LQ optimal control for a double input system described by Equation 7, a performance index  $J$  is defined as:

$$J = \frac{1}{2} \int_0^\infty e^T Q e + R^T U R \quad (8)$$

where  $Q$  and  $R$  positive diagonal weighting matrices so that  $Q = \text{diag}(q_\omega, q_\phi)$ ,  $R = \text{diag}(r, r)$ .

Via LQ method, to find the optimal control law in an infinite period, the Riccati Equation:

$$A^T P + PA + Q - PbR^{-1}b^T P = 0 \quad (9)$$

must be solved. Thus, the control law to yield a minimum performance index is obtained as:

$$U = -(R^{-1}b^T P)e = -Ke = \begin{bmatrix} U_\omega^* \\ U_\phi^* \end{bmatrix} \quad (10)$$

In Equation 9 since  $A$ ,  $b$  and  $R$  are the diagonal matrices, hence  $P$  must also be a diagonal matrix. As a result  $K$  has to be a diagonal matrix too.

$$K = \text{diag} \left[ K_\omega, K_\phi \right] \quad (11)$$

**C. Perturbed System Control** Consider Equation 7 with uncertainties so that

$$\dot{e} = Ae + bU + r(t) \quad (12)$$

where

$$r(t) = \begin{bmatrix} r_\omega \\ r_\phi \end{bmatrix} = \begin{bmatrix} f_\omega + \Delta a_\omega e_\omega + \Delta b_\omega U_T \\ f_\phi + \Delta a_\phi e_\phi + \Delta b_\phi U_\phi \end{bmatrix} \quad (13)$$

In fact  $\Delta A$  and  $\Delta b$  are denoted as the uncertainties introduced by system parameters,  $J$ ,  $B$  and  $K_T$ .  $r(t)$  called, "lumped uncertainty".

Let the system be under linear state feed back control ( $U$ ) described by (10), the closed loop dynamic, in the nominal condition, is verified by

$$\dot{e} = (A - bK)e = A_C e \quad (14)$$

At this stage, the LQ feed back control and SM control are combined in order to design the system control laws capable of reserving an equivalent system dynamic as well as the closed loop dynamic for the perturb system same as the nominal condition.

The SM control objective consists of designing First equilibrium surfaces  $S(e, t) \in R^2$ , such that the state trajectories of the plant restricted to the equilibrium surfaces have a desired behavior in terms of tracking, relation and stability. Secondly, according to the SM reaching condition, the switching control effort  $U_c(e, t)$  is determined so as to be able to curb the state trajectories to the equilibrium surfaces and maintain them on the surfaces so that  $e_\omega$  and  $e_\phi$  (the rotor speed and rotor flux amplitude errors) converge to zero as well as reserve the system trajectories as the nominal condition.

In the classical SM control, the chattering is a bothering problem. To reduce this effect, the SM speed and rotor flux controllers are derived based on using the switching surfaces with integral components, which posses the exponential stability [17].

$$S = \begin{bmatrix} S_\omega \\ S_\phi \end{bmatrix} = [C^T e(t) - e(0)] - C^T A_c \int_0^t e(\tau) d\tau \quad (15)$$

where  $A_c = A - bK^T$  and  $c^T$  are (2\*2) positive diagonal matrix and  $e(0)$  is the initial state of vector  $e(t)$ .

Note that the scalar functions  $S_\omega$  and  $S_\phi$  are decoupled. That is because  $A$  and  $b$  are the

diagonal matrices.

Consider Equation 13, under the nominal condition. It is due to the state feedback given by Equation 10, that the system control posses the sliding surfaces  $S(e,t)=0$  on which the states slide. In addition, since  $S(0)=0$  at  $t=0$ , there is no reaching phase as in the conventional SM control.

Under the influence of uncertainty and disturbance, the perturbed and uncertain system cannot still preserve the system response as the nominal condition; and the system performance under the control of Equation 10, which is designed for the nominal system, is surely degraded. Moreover the minimum performance index cannot be achieved and the sliding condition cannot be maintained either.

To maintain the sliding condition and preserve the nominal system response and performance subjected to the uncertainty and/or external disturbance, additional control effort is required in order to ensure the SM reaching conditions that are described by

$$F\dot{F} < 0 \quad (16)$$

where  $F = \text{diag}(S_\omega, S_\Phi)$ .

To control the states on the sliding surfaces under the system perturbed condition, an extra control effort must be chosen as:

$$U_c = -\rho \text{sgn}(S) \quad (17)$$

Then the total system control is:

$$U = U_C + U_L = -K^T e - \rho \text{sgn}(S) = \begin{bmatrix} U_T^* \\ U_\Phi^* \end{bmatrix} \quad (18)$$

where  $\rho = \text{diag}[\rho_\omega, \rho_\Phi]$ .

The added term,  $-\rho \text{sgn}(S)$ , is the variable structure control for the system and  $S$  is the sliding switching functions described by Equation 15.

Linking Equations 12, 15, 16 and 18, it can be shown that

$$\begin{aligned} S_\omega(t) \cdot \dot{S}_\omega(t) &= [r_\omega - b_\omega \rho_\omega \text{sgn}(S_\omega)] \cdot S_\omega \leq 0 \\ S_\Phi(t) \cdot \dot{S}_\Phi(t) &= [r_\Phi - b_\Phi \rho_\Phi \text{sgn}(S_\Phi)] \cdot S_\Phi \leq 0 \\ &\text{for } t > 0 \end{aligned} \quad (19)$$

Combining Equations 13 with 19 yields

$$\begin{aligned} \rho_\omega &> \left| \frac{1}{(b_\omega - \Delta b_\omega)} (f_\omega + \Delta a_\omega e_\omega + \Delta b_\omega k_\omega e_\omega) \right|_{\max} \\ \rho_\Phi &> \left| \frac{1}{(b_\Phi - \Delta b_\Phi)} (f_\Phi + \Delta a_\Phi e_\Phi + \Delta b_\Phi k_\Phi e_\Phi) \right|_{\max} \end{aligned} \quad (20)$$

Therefore from Equation 20, the lower bands of  $\rho_\omega$  and  $\rho_\Phi$  can be obtained as

$$\begin{aligned} \rho_\omega &= \frac{1}{b_\omega - \beta_\omega} (\varepsilon_\omega |e_\omega| + f_\omega) \\ \rho_\Phi &= \frac{1}{b_\Phi - \beta_\Phi} (\varepsilon_\Phi |e_\Phi| + f_\Phi) \end{aligned} \quad (21)$$

Where

$$\begin{aligned} \Delta b_\omega < \beta_\omega, \quad & \left| \Delta a_\omega + \Delta b_\omega k_\omega \right| < \varepsilon_\omega, \\ \Delta b_\Phi < \beta_\Phi, \quad & \left| \Delta a_\Phi + \Delta b_\Phi k_\Phi \right| < \varepsilon_\Phi \end{aligned}$$

and  $\varepsilon_\omega, \varepsilon_\Phi$  are positive constants. A consequence the curbing condition  $F(t)\dot{F}(t) < 0$  is assured. In addition the closed loop system dynamics for the nominal condition can be obtained, i.e. the system will have its activity like  $\dot{e} = A_c e$  regardless of the existence of disturbance and uncertainty. In view of Equation 15, it is evident that  $S(t) = 0$  at  $t = 0$  and also later than that. Thus, a system controlled by the proposed rotor speed and rotor flux-controllers is in the sliding-mode at the beginning, i.e. the system can have robust properties from the beginning of the control process.

#### 4. SLIDING-MODE OBSERVER

**A. Nonlinear Robust Observer with Discontinuous** Parameters and stator currents and voltages as input variables, is proposed so that the rotor speed and rotor time constant can be estimated simultaneously.

From Equation 1, the following rotor flux observer is assumed:

$$\frac{d}{dt} \begin{bmatrix} \hat{i}_s \\ \hat{\phi}_r \end{bmatrix} = \begin{bmatrix} \hat{A}_{11} & \hat{A}_{12} \\ \hat{A}_{21} & \hat{A}_{22} \end{bmatrix} \begin{bmatrix} i_s \\ \hat{\phi}_r \end{bmatrix} + \begin{bmatrix} \hat{B}_1 \\ 0 \end{bmatrix} v_s - \begin{bmatrix} K \text{sgn}(\tilde{i}_s) \\ 0 \end{bmatrix} \quad (22)$$

where

$$\begin{aligned} \hat{A}_{11} &= - \left( \frac{R_s}{\sigma} + \beta M \hat{\alpha} \right) I, \quad \hat{A}_{12} = \frac{M}{\sigma L_r} (\hat{\alpha} I - \hat{\omega}_r J) \\ \hat{A}_{21} &= M \hat{\alpha} I, \quad \hat{A}_{22} = -\hat{\alpha} I + \hat{\omega}_r J \\ \hat{\alpha} &= \alpha_n + \Delta \hat{\alpha}, \quad K = \begin{bmatrix} k_d & 0 \\ 0 & k_q \end{bmatrix} \end{aligned}$$

where  $\alpha_n$  is the nominal value of  $\alpha$

Combining Equations 1 and 18, gives

$$\frac{d}{dt} \begin{bmatrix} \tilde{i}_s \\ \tilde{\phi}_r \end{bmatrix} = \begin{bmatrix} 0 & A_{12} \\ 0 & A_{22} \end{bmatrix} \begin{bmatrix} \tilde{i}_s \\ \tilde{\phi}_r \end{bmatrix} + \begin{bmatrix} \tilde{A}_{11} & \tilde{A}_{12} \\ \tilde{A}_{21} & \tilde{A}_{22} \end{bmatrix} \begin{bmatrix} i_s \\ \hat{\phi}_r \end{bmatrix} - \begin{bmatrix} K \text{sgn}(\tilde{i}_s) \\ 0 \end{bmatrix} \quad (23)$$

where

$$\begin{aligned} \tilde{i}_s &= \hat{i}_s - i_s, \quad \tilde{\phi}_r = \hat{\phi}_r - \phi_r \\ \tilde{\alpha} &= \hat{\alpha} - \alpha, \quad \tilde{\omega}_r = \hat{\omega}_r - \omega_r \\ \tilde{A}_{11} &= -\beta M \tilde{\alpha} I, \quad \tilde{A}_{12} = \beta (\tilde{\alpha} I - \tilde{\omega}_r J) \\ \tilde{A}_{21} &= M \tilde{\alpha} I, \quad \tilde{A}_{22} = -\tilde{\alpha} I + \tilde{\omega}_r J \end{aligned}$$

Candidating the following positive definite Lyapunov function

$$V = \frac{1}{2} \left( \tilde{\phi}_r^T \tilde{\phi}_r + \frac{1}{c_\omega} \tilde{\omega}_r^2 + \frac{1}{c_\alpha} \tilde{\alpha}^2 \right) \quad (24)$$

Derivating V with respect to time t, yields

$$\begin{aligned} \dot{V} &= -\alpha \tilde{\phi}_r^T \tilde{\phi}_r + \tilde{\omega}_r \left( \frac{1}{c_\omega} \tilde{\omega}_r - (J \hat{\phi}_r)^T \tilde{\phi}_r \right) \\ &+ \tilde{\alpha} \left( \frac{1}{c_\alpha} \tilde{\alpha} - (\hat{\phi}_r - M \hat{i}_s)^T \tilde{\phi}_r \right) \end{aligned} \quad (25)$$

To conserve the observer convergence, it is required to have  $\dot{V} < 0$ . Therefore from Equation 24

$$\dot{\tilde{\omega}}_r = c_\omega (J \hat{\phi}_r)^T \tilde{\phi}_r \quad (26)$$

$$\dot{\tilde{\alpha}} = c_\alpha (\hat{\phi}_r - M \hat{i}_s)^T \tilde{\phi}_r \quad (27)$$

Equations 22 and 23 provide two adaptive laws in order to estimate the rotor speed and rotor time constant simultaneously.

From the IM fifth order model shown in Equation 1, one can show that

$$\phi_r = \frac{1}{\beta} \left( \frac{\phi_s}{\sigma} - i_s \right) \quad (28)$$

Once the estimated error of the stator flux  $\tilde{\phi}_s$  is known, then  $\tilde{\phi}_r$  can be obtained from Equation 27

Using the stator voltage Equation as

$$\dot{\phi}_s = -R_s i_s + v_s \quad (29)$$

The stator flux vector can be estimated as:

$$\dot{\hat{\phi}}_s = -R_s i_s + v_s - K \text{sgn}(\tilde{i}_s) \quad (30)$$

From Equations 26 and 29, the stator flux estimated error is obtained as:

$$\dot{\tilde{\phi}}_s = -K \text{sgn}(\tilde{i}_s) \quad (31)$$

Using a first order low pass filter as [5]

$$\tilde{\phi}_s^{\text{eq}} = \frac{1}{\mu s + 1} \tilde{\phi}_s \quad (32)$$

where  $(\frac{1}{\mu})$  the filter low pass cut-off frequency is sufficiently small enough to allow slow component of the motion but is large enough to eliminate the high frequency component. Combining Equations 27 and 31, the rotor flux estimated error is obtained as

$$\tilde{\phi}_r = \frac{1}{\beta} \left( \frac{\tilde{\phi}_s^{\text{eq}}}{\sigma} - \tilde{i}_s \right) \quad (33)$$

To guarantee the convergent behavior of the estimation laws corresponding to rotor speed and rotor time constant, it is necessary to show that these estimation laws satisfy the persistency of the excitation (PE) condition.

**B. Parameter Convergence** The PE condition implies that if the estimation error dynamic,  $\tilde{\theta}$ , is described as [10]

$$\dot{\tilde{\theta}} = -\Gamma Wx \quad (34)$$

and  $\int_0^t W^T(\tau) W(\tau) d\tau$  is positive definite for some  $T > 0$  and every  $t > 0$ , then, the estimation errors will converge exponentially to zero.

From Equations 25 and 26

$$\tilde{\theta} = \begin{bmatrix} \tilde{\omega}_m \\ \tilde{\alpha} \end{bmatrix}, \quad x = \tilde{\phi}_r, \quad \Gamma = \text{diag}(c_\omega, c_\alpha)$$

$$W = \begin{bmatrix} (J\hat{\phi}_r)^T \\ (\hat{\phi}_r - M i_s)^T \end{bmatrix} \quad (35)$$

and then

$$WW^T = \begin{bmatrix} (J\hat{\phi}_r)^T \\ (\hat{\phi}_r - L_m i_s)^T \end{bmatrix} \begin{bmatrix} J\hat{\phi}_r & \hat{\phi}_r - L_m i_s \end{bmatrix} \quad (36)$$

$$= \begin{bmatrix} (\hat{\phi}_{dr} - L_m i_{ds})^2 + (\hat{\phi}_{qr} - L_m i_{qs})^2 & \hat{\phi}_{qr}(\hat{\phi}_{dr} - L_m i_{ds}) - \hat{\phi}_{dr}(\hat{\phi}_{qr} - L_m i_{qs}) \\ \hat{\phi}_{qr}(\hat{\phi}_{dr} - L_m i_{ds}) - \hat{\phi}_{dr}(\hat{\phi}_{qr} - L_m i_{qs}) & \hat{\phi}_{dr}^2 + \hat{\phi}_{qr}^2 \end{bmatrix}$$

To satisfy the mentioned condition, it is necessary to have  $\text{Det}(WW^T) > 0$ .

$$\text{Det}(WW^T) = [\hat{\phi}_{dr}(\hat{\phi}_{dr} - L_m i_{ds}) + \hat{\phi}_{qr}(\hat{\phi}_{qr} - L_m i_{qs})]^2$$

$$= [\hat{\phi}_r^2 - L_m (\hat{\phi}_{dr} i_{ds} + \hat{\phi}_{qr} i_{qs})]^2 = [\hat{\phi}_r^2 - L_m U_\phi \hat{\phi}_r]^2 \quad (37)$$

Equating 37 to zero, it yields

$$\hat{\phi}_r = L_m U_\phi \quad (38)$$

On the other hand, from Equation 5, it can be concluded:  $\text{Det}(WW^T) = 0$ . Therefore, in steady state conditions under the assumption of a constant rotor flux amplitude  $\text{Det}(WW^T) = 0$  and as a result the PE condition is not satisfactory.

Now consider Equation 23 in a steady state condition and with the assumption of ( $\dot{\tilde{\phi}}_r = \dot{\tilde{\phi}}_r = 0$ )

$$\tilde{\alpha} \cdot (M i_s - \hat{\phi}_r) = -\tilde{\omega}_r \cdot (J\hat{\phi}_r) \quad (39)$$

Equation 39 shows that the steady state error exists in the rotor speed and rotor time constant estimations, even if the stator current and rotor flux estimation errors exponentially converge to zero.

To solve this problem, the rotor flux reference command has to be contained enough in distinct frequencies in order to satisfy PE conditions. Therefore a low frequency low amplitude ac signal is superimposed to the rotor flux reference signal. In our case, the frequency of this signal is 3Hz and its amplitude is about 4% of the rated rotor flux.

One may note that if the aim is only to estimate the rotor speed with tuned rotor resistance ( $\tilde{\alpha} = 0$ ), in this case the P.E. is always satisfactory and hence no need to use a low frequency, low amplitude ac signal.

In our proposed control method, it is assumed that the rotor resistance and rotor speed are unknown constant parameters; such an assumption is reasonable because the dynamics of rotor speed and rotor resistance are slow enough compared to stator voltages and currents dynamics.

## 5. SVM INVERTER

The Space-vector PWM has recently grown in to a very popular PWM method for voltage-fed converter ac drives because it offers the advantages of improved PWM quality and extended voltage range in the under-modulation region. This inverter has a better utilization of dc link voltage, 33% reduction in switching losses, reduced harmonic distortion and lower devices ratings compared to a conventional two level SPWM inverter [11].

A three-level SV-based PWM inverter is employed to feed the induction drive system. The three-level neutral-point inverter has been shown to provide significant advantages over the conventional two-level VSI for high-power applications [11]. The main advantages are as follows: 1. The voltage across the switches is only half the dc bus voltage, and 2. the first group of voltage harmonics is centered around twice the switching frequency thus enabling further reduction in size, weight and cost of passive components. On the other hand this topology also has its disadvantage: (1) this inverter requires a





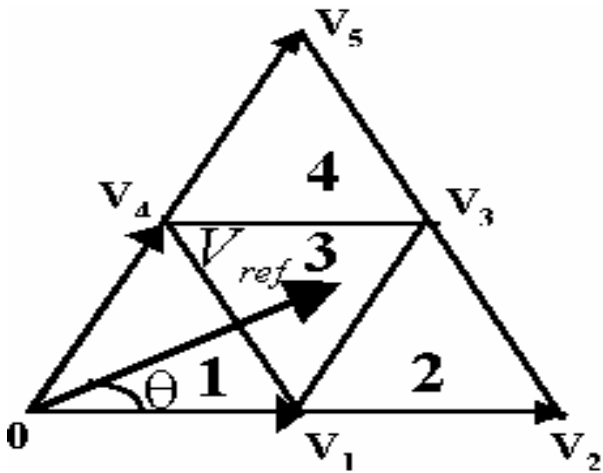


Figure 3. First switching sector.

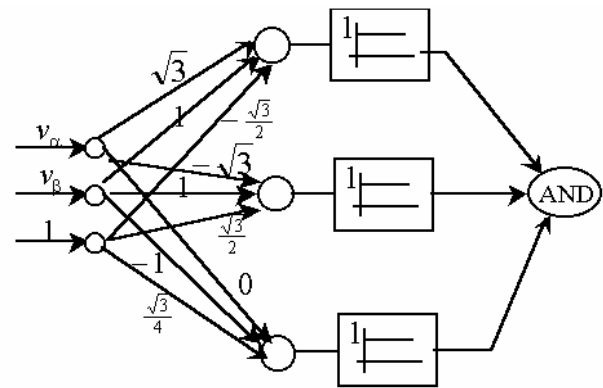


Figure 5. CNN for region # 3.

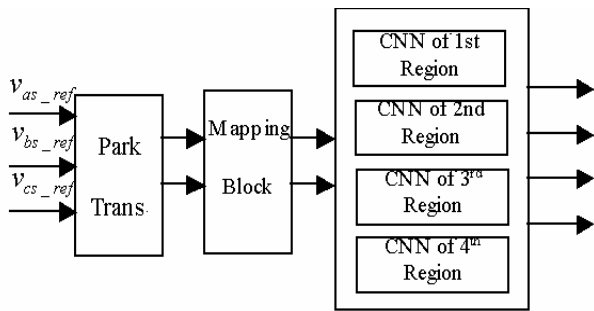


Figure 4. Sector and region detector based on CNN.

example the detailed structure of the third path is shown in Figure 5. The mapping block in Figure 4, maps all other five sectors to sector # 1, by subtracting appropriate multiples of  $\pi/3$  to the phase of  $\underline{V}_{ref}$ .

**C. Neutral point voltage balancing** All available voltage space vectors for 3-level VSIs are shown in Figure 2. Each phase a, b and c can be connected to either positive (P), negative (N), or neutral (O) points of the DC link. Not all the vectors affect the NP balance. The ones that do are summarized in Table 1 [12]. Large vectors do not affect the NP balance because they connect the phase currents to either the positive or negative DC rail, and the NP remains unaffected. Medium vectors connect one of the phase currents to the

TABLE 1. Neutral Point Current.

Positive Small Vectors	$i_{NP}$	Negative Small Vectors	$i_{NP}$	Medium Vectors	$i_{NP}$
ONN	$i_a$	POO	$-i_a$	PON	$i_b$
PPO	$i_c$	OON	$-i_c$	OPN	$i_a$
NON	$i_b$	OPO	$-i_b$	NPO	$i_c$
OPP	$i_a$	NOO	$-i_a$	NOP	$i_b$
NNO	$i_c$	OOP	$-i_c$	ONP	$i_a$
POP	$i_b$	ONO	$-i_b$	PNO	$i_c$

NP, making the NP potential dependent, in part, on the loading conditions. They are the most important sources of the NP potential unbalance. Small vectors come in pairs. Each vector in a pair generates the same line-to-line voltages.

A small vector that connects a phase current to the NP point, without changing the sign of the current, will be referred to as a positive small vector. The other one, connecting the phase current with the negative sign, will be called a negative small vector. The majority of the NP voltage balancing schemes used in SVM relies on some form of manipulation of small vectors in a pair, where the relative duration of positive and negative small vectors in a pair is usually adjusted in order

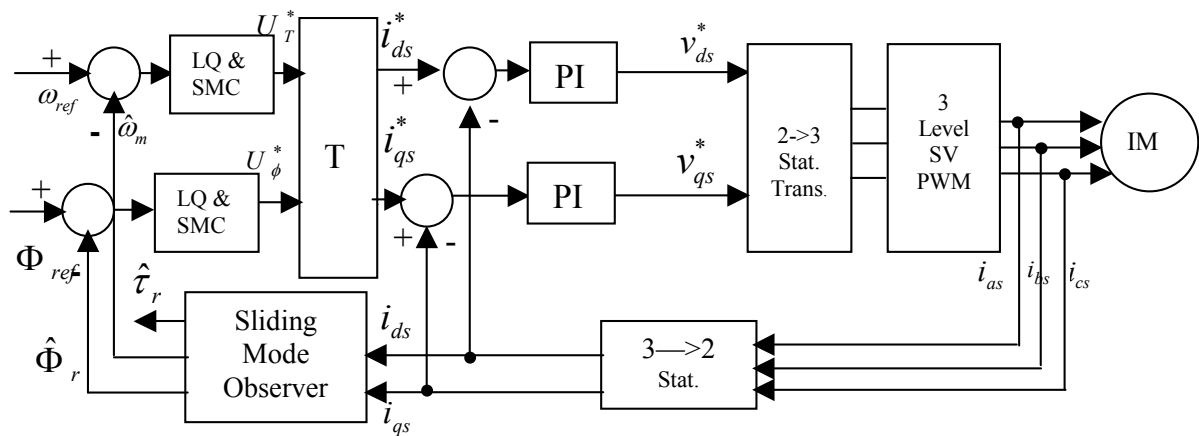


Figure 6. Drive system block diagram.

to compensate for the error in the NP.

In [12], a good review on neutral point dc control is done and active, passive and hysteresis control methods are compared. Passive control, where the positive and negative small vectors are selected alternatively in each new switching cycle, is suggested for perfectly balanced loads. The hysteresis type control is the simplest method for NP control and requires the knowledge of current direction and then a suitable small vector is selected to compensate NP voltage. At last, the active control is a complicate method and requires measurements of NP voltage and phase currents to control current modulation indexes of small vectors. This method increases the switching losses due to additional switching states.

In our case, we use passive control to neutral point balancing, by a symmetric pattern in each switching period.

The voltage of dc link center tap point is given by [12]:

$$V_{\text{center - tap}} = \frac{V_{\text{dc}}}{2} + \frac{1}{C} \int_0^t i_{\text{NP}}(\tau) d\tau \quad (42)$$

## 6. SYSTEM SIMULATION

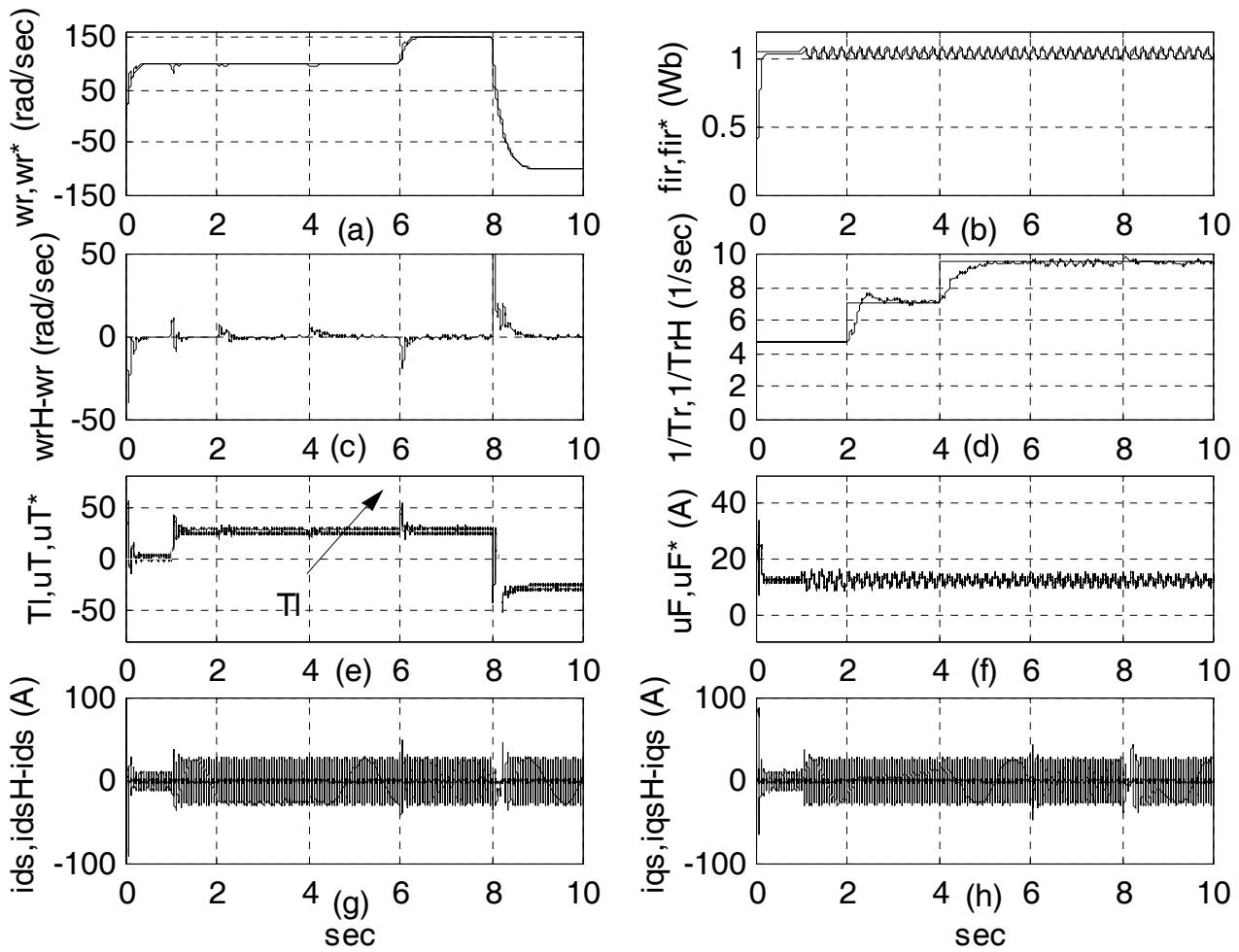
The block diagram of Figure 6 is proposed for closed loop speed sensorless control of the IM drive system.

A C++ computer program was developed to model the machine drive system. A static Runge-Kutta fourth order method was used to solve the system Equations. The effectiveness of the proposed control approach is verified by computer simulation and is tested with parameters shown in Table 2 for a (11kW, 380V, 50Hz), cage rotor IM by computer simulation. For this motor, the coefficients of SM controllers, SM observer and conventional PI regulators are obtained by trial and error method.

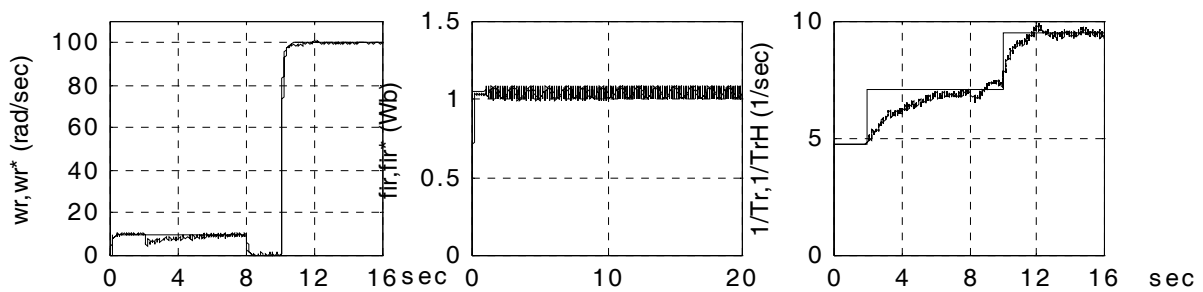
Computer simulation results shown in Figure 7 obtained for an operating condition of  $\omega_r^* = 100\text{rad/sec}$ . (applied at zero second and stepped up to  $150\text{rad/sec}$  at 6sec.),  $T_l = 73\text{N.m}$  at 1sec. ( $R_r = 1.5R_{m}$ , at  $t = 4$  sec) and ( $R_r = 2R_{m}$ , at  $t = 6$  sec.); where  $\omega_r^*$  is the rotor speed reference,  $T_l$  is the motor load torque and ( $R_r, R_{m}$ ) are respectively the rotor actual and rated resistances.

TABLE 2. Motor Parameters.

Power	11 kW	f	50 Hz
$R_r$	.371 $\Omega$	$L_m$	84.2 mH
$R_s$	.415 $\Omega$	$L_r$	87.5 mH
Pole	4	$L_s$	86.9 mH
$B_f$	.00004	$J_m$	.15 $\text{kgm}^2$



**Figure 7.** Drive system performance (a) rotor speed (b) estimated rotor flux (c) rotor speed estimation error (d) estimated rotor time constant (e) torque control signal (f) flux control signal (g,h) stator d and q axis cur.



**Figure 8.** Drive system performance in low speed region (a) rotor speed (b) rotor flux (c) rotor time constant.

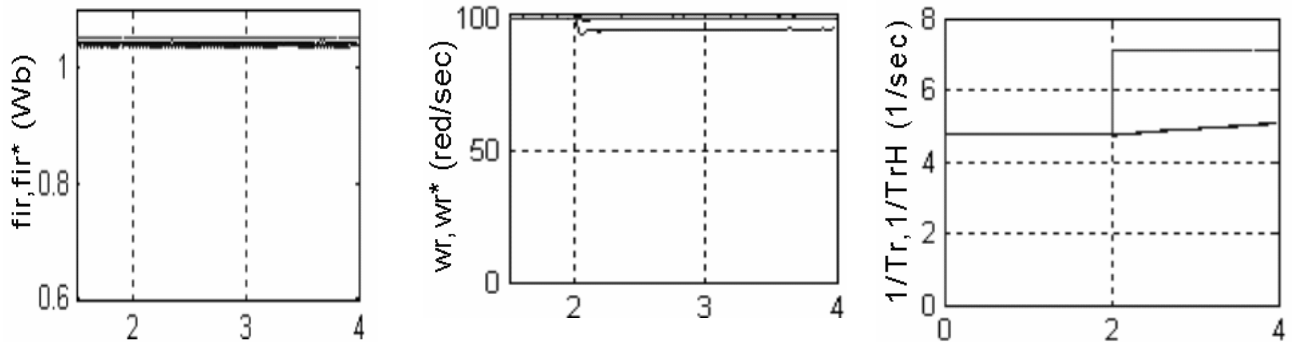


**Figure 9.** Drive performance without an ac signal superimposed to the rotor flux reference command.

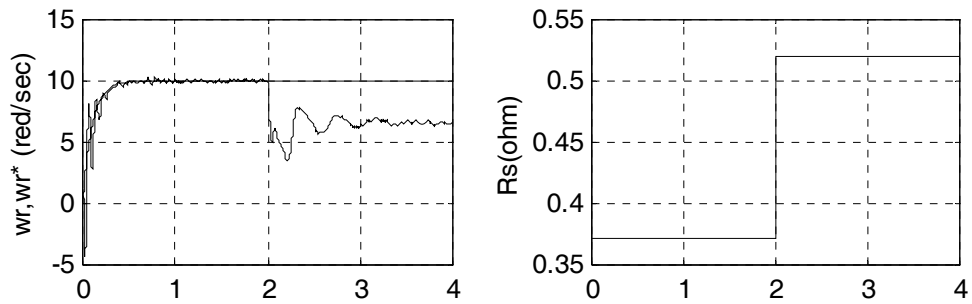


**Figure 10.** Rotor Speed response with stator resistance misestimating.

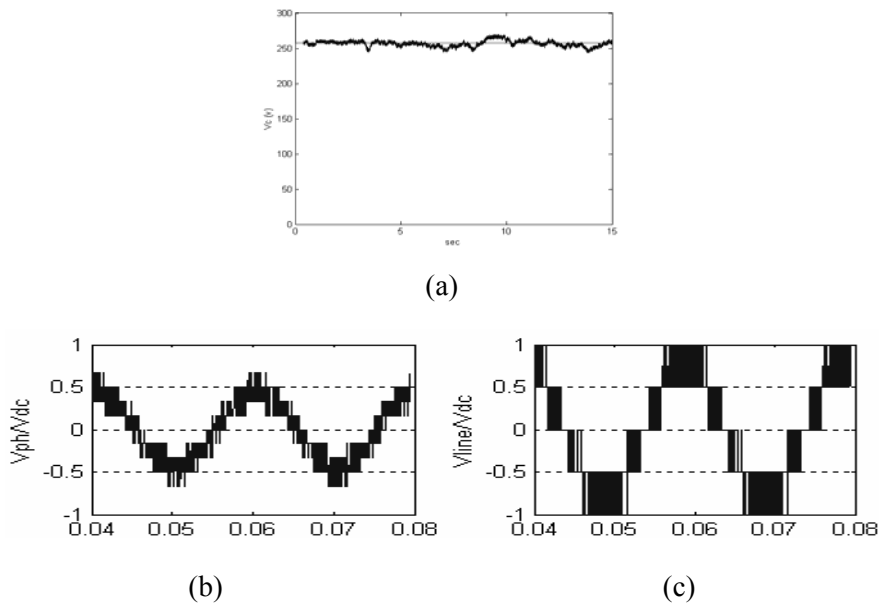


**Figure 11.** Three-level SV based PWM inverter simulation results: (a) voltage of D-link center tap point, (b) phase voltage and (c) line voltage.

From these results, one can see that the proposed system control scheme is robust and stable, subject to the motor parameter uncertainties and motor load torque disturbance. In addition, the rotor speed, rotor time constant, stator currents and estimated rotor flux magnitude track their objective reference values.

Some slow oscillations seen on the motor estimated quantities are due to the low-frequency ac signal component that superimposed on the rotor flux reference command ( $\phi_r^*$ ) in order to satisfy the P.E conditions. Moreover, from computer results obtained, the decoupling between the torque dynamic and dynamic of the rotor flux magnitude is quite obvious. That is because of the torque and rotor flux control states ( $U_T, U_\phi$ ), which perfectly track their respected reference signals ( $U_T^*, U_\phi^*$ ). Moreover, the drive system performance in the low speed region can be seen in Figure 8. These results are obtained for ( $\omega_r^* = 10\text{rad/sec}$ , applied to zero sec, stepped down to zero at 8sec and stepped up to 100rad/sec at 10sec.) for ( $R_r = 1.5R_m$ , at  $t = 4 \text{ sec.}$ ), ( $R_r = 2R_m$ , at  $t = 6 \text{ sec.}$ ) and ( $B = 3B_n, J = 3J_n$ , at 10sec.)

Figure 9 shows that for constant rotor flux amplitude, the PE conditions are not satisfied. As a result the steady-state error is expected in the rotor speed and rotor time constant estimations.

Furthermore the stator resistance variation affects the performance in the IM low speed operating region is as shown especially in Figure 10.

Finally, simulation results obtained corresponding to three-level SV-based PWM inverter are given in Figure 11.

## 7. CONCLUSIONS

Based on partial feedback linearization control, using the induction machine Equations in a stator  $\alpha - \beta$ : fixed axis reference frame, the dynamics of the IM torque and rotor flux modulus have been decoupled first.

Combining SM control and LQ feedback control methods, the composite speed and rotor

flux controllers have been derived to make the IM states follow their nominal trajectory as obtained by the LQ controllers. An SM rotor flux observer has been developed in order to provide the estimation of rotor speed, rotor time constant and the  $\alpha - \beta$ : axis rotor flux components simultaneously. The stability of this observer is proved by Lyapunov stability theory. A three-level SV-based PWM inverter has been employed that feeds the IM drive system. This inverter compared to conventional two-level PWM inverter, has a better utilization of the dc link voltage with less torque pulsation assuming the same switching frequency.

A low frequency, low amplitude ac signal is superimposed to rotor flux reference command, in order to satisfy the persistency of excitation condition.

Computer simulation results obtained have shown the validation of the proposed control approach. However these results have shown that for further improvement of the IM drive system robustness, especially in low speed operating regions, it is also required to estimate the stator resistance parameter. This needs more research which is out of the scope of the present paper.

## 8. REFERENCES

1. Do Ki, S., Sangwonwnich, S., et al., "Implementation of speed-sensorless field oriented vector control using adaptive sliding observers", in *Proc. IEEE IECON'92*, (1992), 453-458.
2. Utkin, V. I., "Sliding mode control design principles and applications to electric drives", *IEEE Trans. Ind. Elect.*, Vol. 40, No. 1, (Feb. 1993), 23-36.
3. Benchaib, A., Rachid, A., Audrezet, E. and Tadjine, M., "Real-time sliding-mode observer and control of an induction motor", *IEEE Trans. Ind. Appl.*, Vol. 46, No. 1, (Feb. 1999), 128-138.
4. Tursini, M., Peralla R. and Parasiliti, F., "Adaptive sliding mode observer for speed-sensorless control of induction motors", *IEEE Trans. Ind. Appl.*, Vol. 36, No. 5, (Sept. 2000), 128-137.
5. derdiyok, A., Guven, M., Rahman, H., Inanc, N., Xu, L., "Design and implementation of a new sliding-mode observer for speed-sensorless control of induction machine", *IEEE Trans. Ind. Elect.*, Vol. 49, No. 5, (Oct. 2002), 1177-1182.
6. Kubota, H., Matsuse, K., "Speed sensorless field-oriented control of induction motor with rotor resistance adaptation", *IEEE Trans. Ind. Appl.*, Vol. 30, No. 5,

- (Sep.-Oct. 1994), 1219-1224.
7. Tajima, H., Guidi, G. and Umida, H., "Consideration about problems and solutions of speed estimation method and parameter tuning for speed-sensorless vector control of induction motor drives", *IEEE Trans. Ind. Appl.*, Vol. 38, No. 5, (Sep.-Oct. 2002), 1282-1289.
  8. Mondal, S. K., Pinto, J. and Bose, B. K., "A neural-network-based space-vector PWM controller for a three-level voltage-fed inverter induction motor drive", *IEEE Trans. Ind. Appl.*, Vol. 38, No. 3, (May-June 2002).
  9. Wai, R. J., "Adaptive sliding-mode control for induction servo motor drive", *IEE Proc. Electr. Power. Appl.*, Vol. 147, No. 6, (Nov. 2000), 553-562.
  10. Marino, R. and Tomei, P., *Nonlinear Control Design-Geometric, Adaptive and Robust*. Englewood Cliff, NJ: Prentice-Hall, (1995).
  11. Bakhshai, A. R., Saligheh Rad, H. R. and Joos, G., "Space vector Based on classification method in three-phase multi-level voltage source inverters", *IEEE Proc.*, (2001), 597-602.
  12. Celanovic, N. and Boroyovich, D., "A comprehensive study of neutral-point voltage balancing problem in the three-level neutral-point-clamped voltage source PWM inverters", *IEEE Trans. on Power Electr.*, Vol. 15, No. 2, (March 2000).